CHARGE EXCHANGE RECOMBINATION DETECTION OF LOW-Z AND MEDIUM-Z IMPURITIES IN THE EXTREME UV USING A DIGITAL LOCK-IN TECHNIQUE

by
N.H. BROOKS, K.H. BURRELL, R.C. ISLER,
O. MEYER and N.A. PABLANT

JUNE 2010

GENERAL ATOMICS

DISCLAIMER

GA–A26727

CHARGE EXCHANGE RECOMBINATION DETECTION OF LOW-Z AND MEDIUM-Z IMPURITIES IN THE EXTREME UV USING A DIGITAL LOCK-IN TECHNIQUE

by
N.H. BROOKS, K.H. BURRELL, R.C. ISLER,*
O. MEYER† and N.A. PABLANT‡

*Oak Ridge National Laboratory, Oak Ridge, Tennessee USA
†ITER Organization, St Paul Lez Durance Cedex, France
‡University of California-San Diego, La Jolla, California USA

GENERAL ATOMICS ATOMICS PROJECT 30200
JUNE 2010

GENERAL ATOMICS

ABSTRACT

More sensitive detection of charge exchange recombination lines from low-Z elements, and first-time detection from the medium-Z elements nickel and copper, has been achieved in DIII-D plasmas with a digital lock-in technique. That portion of the extreme UV (EUV) spectrum varying synchronously in time with the square-wave modulation of a high energy, neutral heating beam is extracted by forming a scalar product of a correlation function with the data record of each pixel in the linear array detector. The usual, dense array of collisionally excited, metallic lines from the tokamak plasma are strongly suppressed, leaving only a sparse spectrum of lines dominated by charge exchange recombination transitions from fully stripped, low-Z elements. In plasmas with high metal content, charge exchange recombination lines from the Li-like ions of nickel and copper have been positively identified.

I. INTRODUCTION

Application of digital lock-in techniques to extract that portion of the extreme UV (EUV) signal varying synchronously with the modulation of a high energy, neutral beam provides a sensitive new tool for identification and quantification of charge exchange recombination (CER) emissions. Prompt optical emission resulting from charge transfer between the energetic atoms in injected neutral beams and highly ionized impurities in the plasma core was first exploited for plasma diagnostic purposes in the vacuum UV.[1] Soon thereafter, CER lines from $\Delta n = 1$ transitions between high n-values were detected in the more technologically accessible portion of the spectrum above air cutoff; measurements in the visible of line shape and line shift soon yielded ion temperatures and rotational velocities of low-Z core ions.[2–4] The present work marks a return to the ultraviolet, where EUV survey spectrometers enable simultaneous monitoring of many different elements in the plasma core and the low reflectivity of materials in this wavelength region obviates the need for viewing dumps.

II. DIGITAL LOCK-IN METHOD

Square-wave modulation of heating beams on the DIII-D tokamak[5] provides a means to distinguish plasma emission caused by charge exchange recombination processes from that due to collisional processes. The DIII-D beams are repetitively switched between full ON and full OFF, with the OFF time between pulses no shorter than 5 ms. Though slower modulation frequency is sometimes requested, 50 Hz is the value employed most frequently for diagnostic purposes on DIII-D.

As shown in Fig. 1, the EUV survey spectrometer on DIII-D, a dual-range SPRED[6] instrument manufactured by McPherson, Inc., views the 30-Left neutral beam along a tangential path through the plasma column. The solid black bar indicates the trajectory of the 30-Left beam, the bar's thickness corresponds to the 1/e width of the Gaussian-shaped beam cross-section at the vessel midplane. The EUV spectrometer intersects the beam at a major radius $R = 1.88$ m, corresponding to a normalized radius of 0.3 for typical DIII-D plasma shapes
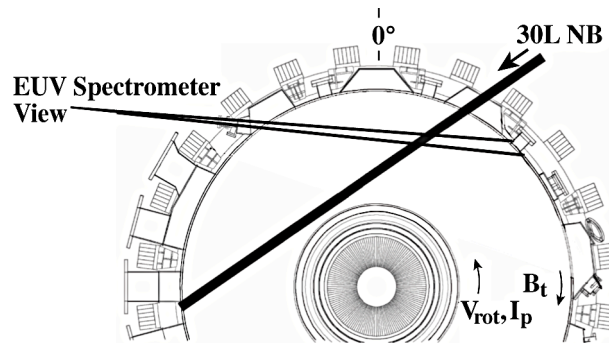

FIG. 1. Crossed geometry of EUV spectrometer and injected neutral beam.

Differencing of consecutive ON/OFF beam phases has been successfully employed in the visible for CER spectroscopy and, more recently, for 2D imaging of CER emission and 2D imaging of beam emission.[7] Cancellation in the background light can be poor, however, when sudden light spikes occur in an unpaired fashion during ON or OFF phases of the beam, as is the case in H-mode confinement plasmas with edge localized modes (ELMs). This problem is much less of a concern in the EUV, since radiation at these short wavelengths is dominated by highly ionized impurities, rather than the low-charge-state impurity ions and neutral hydrogen whose visible emission is enhanced during an ELM.

Digital lock-in improves rejection of quasi-steady-state emission compared with differencing single ON/OFF frame pairs, because better photon statistics are achieved. Also, by averaging over many modulation cycles, digital lock-in leads to a cancellation of randomly occurring ELM light spikes, provided the frequency of the ELMs is much higher, or lower, than the beam modulation frequency.

Traditional Fourier transform techniques, which extract the signal in a narrow frequency band about a single well-defined frequency of modulation, are not optimal for capturing a square wave signal whose Fourier decomposition includes the fundamental frequency, and multiple harmonics ranging up in frequency to the data sampling rate of each pixel in the spectrometer's detector. Speed of spectrometer data acquisition rather than sharpness in the leading edge of the neutral beam pulses, sets the noise floor achievable with this technique. That's because the spectrometer framing rate of 500 Hz is much lower than the 10 kHz frequency response of the neutral beam's ion source. An additional challenge for lock-in analysis comes from the fact that beam modulation within a single DIII-D discharge often consists of several consecutive pulse trains, each train having a different frequency and duty cycle.

The approach adopted here utilizes a correlation function, $CF(t)$, that integrates to zero, by design, over each modulation cycle of the beam (Fig. 2). Period and duty cycle are determined for each pulse train in the beam modulation sequence, *post facto*, by analysis of the 4 kHz command signal applied to the acceleration grid of the beam ion source. During the pulse-ON phase of the command signal, the $CF(t)$ waveform is assigned an amplitude of +1; during the OFF-phase, an amplitude of −1 if the duty cycle is 50%. To minimize drift in the background caused by evolution in plasma conditions during long beam-OFF periods at low duty cycle, the negative parts of the CF waveform are made the same length as the beam-ON periods, i.e., a duty cycle of 50% is imposed for the lock-in analysis whenever the actual duty cycle is less than 50%. When the duty cycle is greater than 50%, the $CF(t)$ waveform is given a negative amplitude greater than one during the OFF-phase, such that $CF(t)$ sums to zero over each modulation cycle.
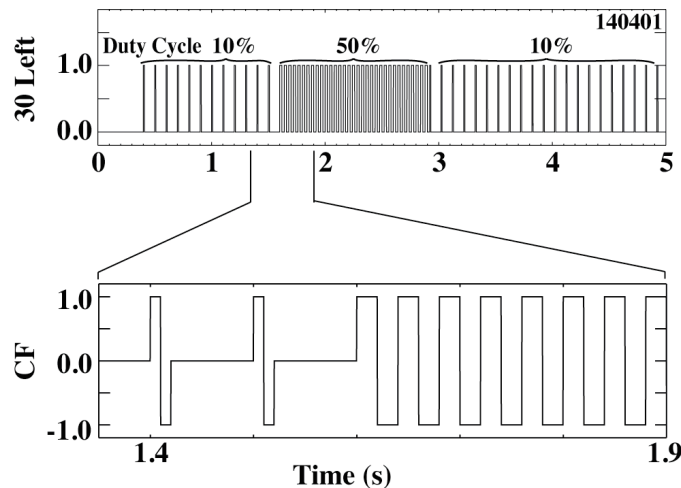

FIG. 2. Neutral beam command signal with three sequential pulse trains of differing frequencies and duty cycles. The expanded trace below is its correlation function: it contains positive and negative phases of equal duration.

Generally, SPRED integration periods and beam modulation periods begin simultaneously, i.e., the SPRED integration periods do not straddle beam-ON and beam-OFF phases. In the rare instances when beam programming gives rise to a non-integral ratio of SPRED sample frequency and beam modulation frequency, the correlation function $CF(t)$ is zeroed during SPRED periods straddling ON/OFF transitions and its offset during OFF-phase frames is adjusted appropriately.

Occasionally, a beam pulse in a long train may be much shorter than its commanded length. Such a shortened or "blocked" beam pulse occurs when the beam protection circuitry detects the occurrence of an arc between grids in the ion source and, subsequently, crowbars the acceleration voltage to zero. Blocked pulses are readily detected by comparing the command waveform with the actual grid voltage signal. Blocked pulses are incorporated into the correlation function with an ON-phase duration and OFF-phase offset different from that of the modulation train in which they occur. Once corrected for beam blocks, the correlation function $CF(t)$ is mapped from the 4 kHz time base of the command signal to the coarser, 500 Hz time base of the SPRED data array.

The SPRED lock-in spectrum is obtained by performing a scalar product of the two temporal vectors $CF(t)$ and $I_j(t)$, for each pixel j. Here, the vector $I_j(t)$ is the SPRED's intensity time history at wavelength λ_j. Only light which varies synchronously with the modulation of the beam is retained in the scalar product $CF(t)*I_j(t)$.

III. LOCK-IN SPECTRA OF LOW-Z ELEMENTS

In Fig. 3(a), the EUV spectrum from a single frame at 2 s is compared with the lock-in spectrum averaged over the period 1.9–2.1 s. Because of the high density of spectral lines from carbon, oxygen and metals in the region 10–20 nm, individual peaks appear to sit atop a quasi-continuum. The impact-excited, resonance lines of the Li-like and Be-like charge states of nickel stand out clearly. By way of contrast, the digital lock-in spectrum contains only a limited number of well-isolated lines, the majority of which can be readily identified with CER transitions in C and O.

The lock-in peaks in the EUV result from the combination of charge transfer into high n-levels, followed by a cascade of the bound electron down through the Rydberg levels. Though most features visible in the lock-in spectrum are a consequence of charge transfer excitation, collisional excitation of resonance lines can become correlated with the beam modulation when the target plasma density is very low and beam injection grossly alters the impurity charge state distribution. In the unusual case in which charge transfer in the beam path lowers the dominant ionic state of a given impurity below H-like, the resonance lines of the H-like charge state suffer a drop in intensity during the beam ON-phase, leading to a negative correlation.

The lock-in spectra of Fig. 3(b) and 3(c) come from the first and last shots, respectively, of the first plasma run day following boronization of the vessel, a process in which diborane gas is decomposed in a helium glow discharge to form a boron coating of roughly monolayer thickness on the plasma-facing wall. These spectra represent the lock-in average over the full, 3.6 s period of beam modulation.

At the start of the day [Fig. 3(b)], the n-2 series of boron can be followed up to an n-value of 6 and the n-1 series of helium up to $n = 7$. Over the course of 23 discharges run that day, the helium line brightness fell by roughly a factor of 20 as helium, trapped in the graphite tiles below the boron film, escaped. Erosion of the boron monolayer led to a recovery in the carbon line intensities which, at the start of the day, were unusually low.

The spectrum from the end of the clean-up day [Fig. 3(c)] is dominated by CER lines of carbon and oxygen; the lines of boron and helium are relatively weak in comparison. The n-2 Rydberg series of carbon can be followed up to an n value of 9, the n-3 series of oxygen up to $n = 10$. For the strongest of the peaks, O 3-2, C 4-2 and C 5-2, second order grating images are weakly visible at twice the wavelengths of the lines. As a consequence of the boron deposit overlying the graphite tiles and exposed metal surfaces, all the discharges on the clean-up day were characterized by extremely low concentrations of metal and, therefore, constitute reference spectra in which the spectral features can be attributed entirely to low-Z elements.

Charge Exchange Recombination Detection of Low-Z and Medium-Z Impurities
in the Extreme UV Using a Digital Lock-In Technique
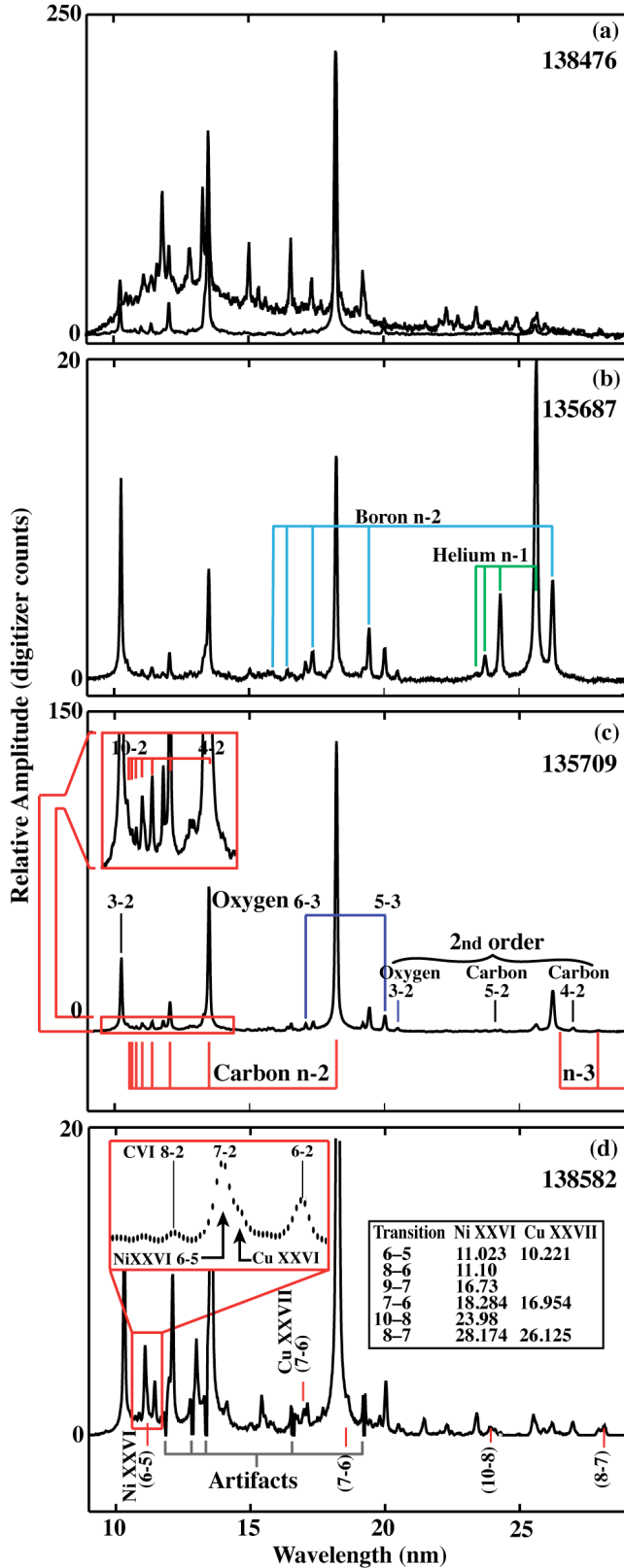
N.H. Brooks et al.

FIG. 3. Lock-in spectra for different plasma conditions in DIII-D: (a) overlay of CER spectrum obtained with digital lock-in (bottom trace), and crowded spectrum without (top trace); (b) first discharge with beams following boronization. Prominent Rydberg series lines from helium and boron are labeled; (c) 23 discharges later on the same run day. Rydberg series lines of carbon and oxygen are labeled, as well as the second order images of their n-2 transitions; (d) discharge with high concentration of nickel and copper. The five negative-going artifacts indentified in the figure occur at the wavelengths of strong nickel resonance lines; they are caused by localized charge depletion in the microchannel plate (MCP) which forms the first stage of the two-stage EUV detector system. In the exploded view of the region 10.5–11.5 nm, the three peaks and the shoulder on the brightest peak have wavelengths of [10.8, 11.02, 11.39] and 11.10 nm, respectively.

Calibration of the relative sensitivity versus wavelength of the SPRED spectrometer on DIII-D was performed using a method based on the calculated intensity ratios among $\Delta n = 1$ and $\Delta n = 2$ CER transitions in He, C, O and Ne.[8] The ease and the accuracy with which these intensity ratios can be extracted with the neutral beam lock-in technique have prompted effort to extend this work to other low-Z elements, such as lithium, boron and fluorine, all of which have been injected into DIII-D in past campaigns. Work is underway, using a beam attenuation code, to relate the absolute intensities of these CER lines to concentrations of the parent impurity charge state at the radius of observation along the beam path. In the case of the low-Z elements He, B, C and O, the parent ion is the fully stripped species.

N.H. Brooks et al.
Charge Exchange Recombination Detection of Low-Z and Medium-Z Impurities
in the Extreme UV Using a Digital Lock-In Technique

IV. LOCK-IN SPECTRA OF MEDIUM-Z METALS

In discharges with unusually high concentrations of nickel and copper, the primary metallic impurities in DIII-D plasmas, the lock-in spectra exhibit beam-correlated features not associated with the usual low-Z impurities. The spectrum in Fig. 3(d) comes from such a shot. The resonance lines from Be-like and Li-like ions of nickel and copper were unusually bright. Four CER lines from Ni XXVI and one from Cu XXVII have been positively identified in the lock-in spectrum: the Δn transitions [(6-5), (7-6), (8-7), (10-8)] in Ni and (7-6) in Cu. The wavelengths of these features match predictions given by relativistic calculations[9] for H-like ions of equivalent net charge, assuming no l-mixing as the population of CX-excited states cascade down in n-level. Bright lines from low-Z elements obscure the other $\Delta n = 1$ and $\Delta n = 2$ CER transitions of nickel and copper in this spectral range. The 6-5 transition in nickel is the brightest, but it is nearly coincident in wavelength with the carbon 7-2 peak. Also, as evident in the expanded view of the region 10.5–11.5 nm, the resonance line of Be-like Cu at 11.12 nm forms a shoulder on the red side of this feature.

From least squares fitting to the known CER features in the lock-in spectrum, wavelengths were deduced for the blended Ni 6-5 peak/C VI 7-2 peak and the shoulder due to copper. A triple Gaussian was employed to model the instrumental line profile.

In Fig. 4, the time history of the feature at 11.02 nm, after correction for the underlying 7-2 transition of C VI, is compared with those of collisionally excited lines from Ni XXVI and Cu XXVII. The CER traces for the CER transitions have poorer time resolution, because each point is deduced from the average over a single beam modulation cycle. It should be noted that detection of visible CER lines from intrinsic vessel metals was achieved in the TFTR tokamak,[10] but low sensitivity did not permit much time resolution within a discharge.
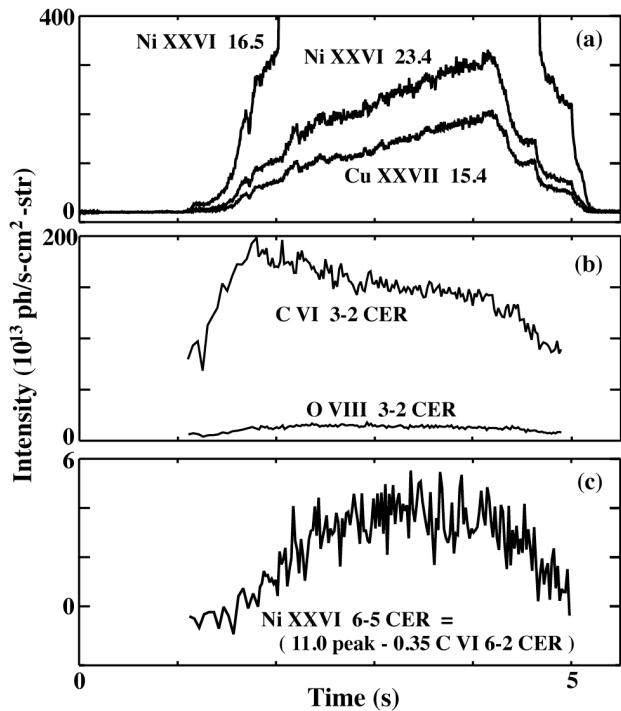

FIG. 4. Time histories of spectral lines in a discharge with high metal content: (a) collisionally excited lines and (b,c) CER transitions, time-averaged over each modulation cycle. The bright Ni XXVI line at 16.5 nm in (a) saturates the detector above 400 ph/s-cm^2-str as a consequence of localized charge depletion in the MCP.

N.H. Brooks et al.
Charge Exchange Recombination Detection of Low-Z and Medium-Z Impurities
in the Extreme UV Using a Digital Lock-In Technique

V. SUMMARY

Digital lock-in to ON/OFF modulation of a DIII-D neutral heating beam has been employed to isolate that portion of the EUV spectrum which varies synchronously with beam injection. By strongly suppressing metallic line emissions caused by collisional excitation, the application of this method makes CER features from low-Z and medium-Z elements much easier to discern. In H-like ions of low-Z elements, long Rydberg series are readily visible. First time detection in the EUV of CER lines from Li-like nickel and copper has been enabled by the high sensitivity of this technique. In addition to providing a sensitive tool for determining concentrations of highly ionized impurities in the plasma core, the method lends itself to improvement of intensity calibration using calculated ratios of intensity ratios among $\Delta n = 1$ and $\Delta n = 2$ CER transitions.

REFERENCES

[1] R. C. Isler, Phys. Rev. Lett. **38**, 1359 (1977).

[2] R. J. Fonck, R. J. Goldston, R. Kaita, and D. E. Post, Appl. Phys. Lett. **42**, 239 (1983).

[3] R. C. Isler and L. E. Murray, Appl. Phys. Lett. **42**, 355 (1983).

[4] R. J. Groebner, N. H. Brooks, K. H. Burrell, and L. Rottler, Appl. Phys. Lett. **43**, 920 (1983).

[5] J. L. Luxon, Nucl. Fusion **42**, 614 (2002).

[6] R. J. Fonck, A. T. Ramsey and R. V. Yelle, Appl. Optics **21**, 2115 (1982).

[7] M. A. Van Zeeland, J. H. Yu, N. H. Brooks, W. W. Heidbrink, K. H. Burrell, R. J. Groebner, A. W. Hyatt, T. C. Luce, N. Pablant, W. M. Solomon, M. R. Wade, Plasma Phys. Control. Fusion **52**, 045006 (2010).

[8] R. C. Isler and R. A. Langley, Appl. Opt. **24**, 254 (1985).

[9] G. W. Erickson, J. Phys. Chem. Ref. Data **6**, 831 (1977).

[10] R. J. Knize, R. J. Fonck, R. Howell, R. A. Hulse, K. P. Jaehnig, Rev. Sci. Instrum. **59**, 1518 (1988).

ACKNOWLEDGMENT